

## Constructal Design of Weight Optimized Metal Hydride Storage Device Embedded with Ribbed Honeycomb

Martin George and G. Mohan\*

Centre for Computational Research in Clean Energy Technologies  
Sree Chitra Thirunal College of Engineering  
Thiruvananthapuram-695018, Kerala, India.  
Email: mohan.g.menon@sctce.ac.in

### Abstract

Hydrogen is considered as the potential energy carrier of future automobiles. However safety and low charging rates are some of the major challenges to be addressed. Compared to high pressure storage, solid state storage in metal/complex hydrides offers several advantages. Heat transfer is the major limiting factor affecting hydrogen sorption in metal hydride storage devices. Different heat transfer enhancement methods are reported in literature. However most such studies do not propose a weight optimized design for the given capacity and charging rate. The proposed constructal design of the storage device with multiple heat exchanger tubes integrated with ribbed honeycomb can effectively transport sorption heat to the coolant in the most effective manner analogous to bio transport systems. The numerical study on the parametric influence of the proposed device on sorption performance is conducted in COMSOL Multiphysics.

**Keywords:** Complex hydride, Heat and mass transfer, Constructal design, Simulation, Hydrogen storage

### 1. Introduction/Background

Sodium alanate is one of the promising materials for the storage of hydrogen which offers high gravimetric capacity. The sorption kinetics of alanates can be improved by mechanical grinding and chemical doping of alloys. Sodium alanate so modified are capable of reversible storage of hydrogen upto 3.0 wt. % at 80–140°C and about 4.5–5 wt. % when operated at temperatures around 150–180°C.

Even though, complex hydrides offer the benefit of high gravimetric storage capacity, their low effective thermal conductivity and high sorption heat are major shortcomings. Different methods to improve thermal conductivity of metal hydrides such as inserts, foams, wires and compacts [1] can be employed to complex hydrides with suitable modifications. However such studies are rarely reported. Hardy and Anton [2, 3] have proposed models to study the sorption performance of shell and tube type hydrogen storage device (with and without fins) containing  $TiCl_3$  catalyzed  $NaAlH_4$ . The charging rate of finned storage device was found to be better than that without fins due to enhanced heat transfer. Raju and Kumar [4] studied the performance of hydrogen storage device with internal tubes and fins to meet the drive cycle demand of fuel cell for different operating conditions.

Maha Bhouri et al. [5] studied the heat and mass transfer of multi-tubular sodium alanate based finned reactor. They found that the charging of the system can be improved if cooling tubes with hexagonal cross-section were employed. The parametric study by the same authors [6] reported the superior hydrogenation performance of sodium alanate based multi-tubular storage device equipped with longitudinal fins.

The above studies validate the effectiveness of high conductivity fins embedded with intermetallic/complex hydrides to improve the heat and mass transfer performance of the device. However, their configuration and sizing are important factors to derive the best performance of the device. Lozano et al. [7] studied the effects of heat transfer on the sorption kinetics of complex hydride reacting systems with different cell sizes. For larger cells, the sorption rate decreases due to low heat transfer. Therefore, heat liberated in the alloy during hydrogenation needs to be removed by suitable configuration of high conductivity paths. This can be inserted into cylindrical, liquid cooled, storage device with multiple HX tubes, as reported by Mohan et al. [8, 9] for metal hydrides. In the present study, a constructal design of aluminum honeycomb with interconnected ribs is proposed for heat transfer enhancement of cylindrical storage device with multiple heat exchanger tubes. The present study deals with the effect of salient geometric parameters on the hydrogenation performance of the device. The device can be weight optimized for the most favourable performance.

## 2. Physical Model

Figure 1 shows the schematic of the cylindrical liquid cooled hydrogen storage device with  $\text{TiCl}_3$  catalyzed  $\text{NaAlH}_4$  used as the storage material. The device is embedded with ribbed aluminium honeycomb. The honeycomb imparts good heat transfer properties, light weight and structural integrity to the device. Each honeycomb cell consists of a central cooling tube surrounded with arteries for hydrogen gas supply. Coolant is circulated through the cell centred tubes to transport the sorption heat.

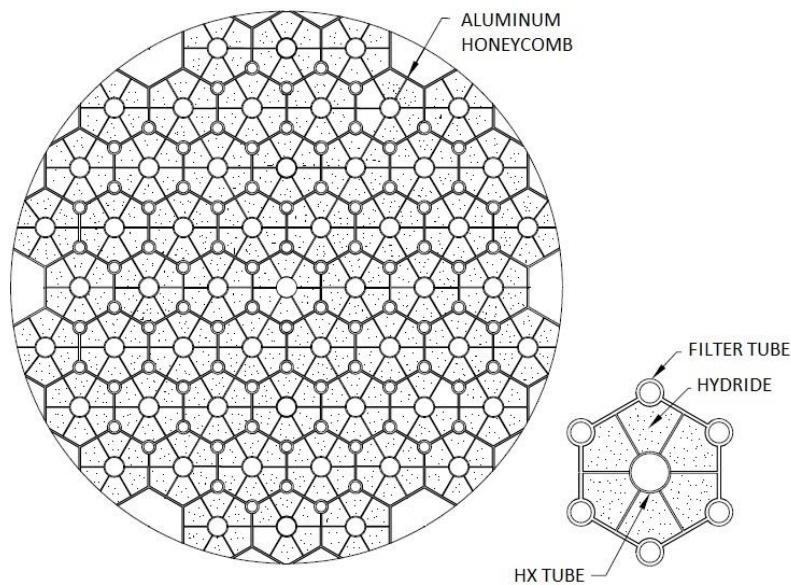
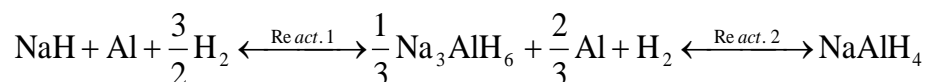


Fig. 1 Schematic of liquid cooled hydrogen storage device embedded with aluminium honeycomb

Hydrogen supplied to the alloy bed causes the reaction to begin, which generate enormous heat. The honeycomb with the associated cooling tubes removes the heat to enhance sorption rate. The hydrogen absorption in the alloy bed consists of two successive reactions as given below.



### Constructal Design

The device with the multiple honeycomb cells can be considered as a constructal arrangement for heat removal. The cell walls acts as primary channels for heat transfer from the alloy bed, which are located at the regions with maximum possible temperature. Ribs are secondary channels which transport this heat to the central tube through which coolant is circulated. One side of the honeycomb wall connected to the respective rib can be considered as a T-fin which is shown in Fig. 2. Every cell consists of six such T-fins connected to the central tube. The optimized dimensions of these T-fins correspond to the minimum heat flow resistance which needs to be determined.

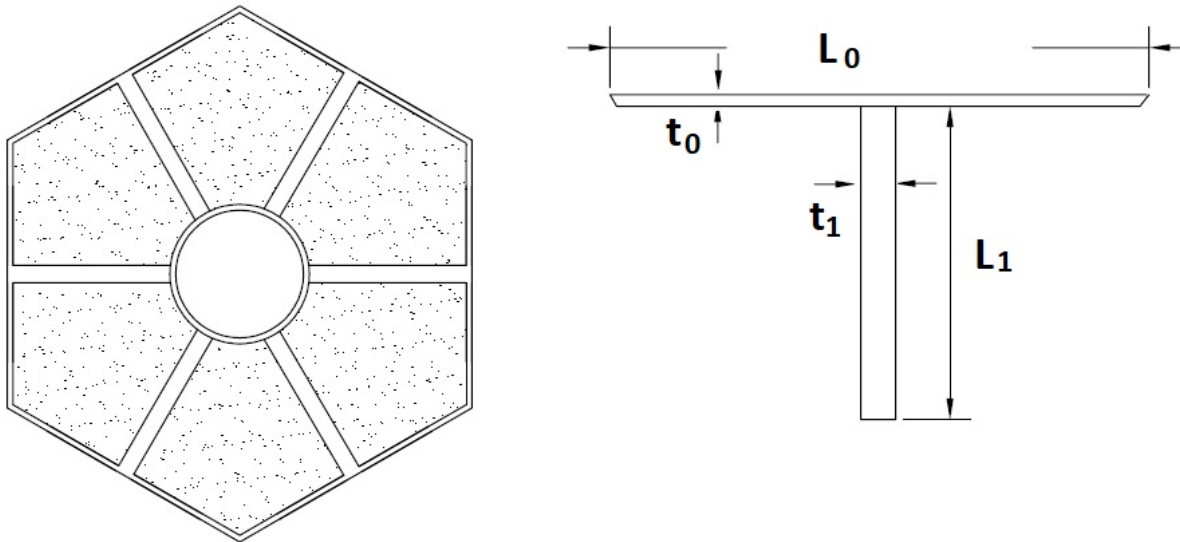


Fig. 2 Schematic of hexagonal cell for simulation as assembly of T shaped fins

### 3. Problem Formulation

The important assumptions used to simplify the formulation of the mathematical model are given below.

1. Coolant flow in the tubes is such that the channel walls are isothermal.
2. Adequate numbers of gas supply filters is provided to keep the gas pressure drop negligible.
3. Hydride temperature is moderate and therefore convection and radiation effects are neglected.
4. The effect of volumetric expansion/contraction of the bed is not accounted [10].
5. Local thermal equilibrium exists in the bed.
6. The powder bed is homogenous and isotropic. The effect of parameters such as void fraction, thermal conductivity and mass diffusivity are independent of position.
7. The bed porosity changes are negligible with the number of charge-discharge cycles [10].
8. The hydride is duly packed in the container to avoid any gaps and the thermal contact resistance is negligible.

The conservation equations for the reaction bed are as given below.

#### Mass Balance

The mass conservation equation of different hydride species in polar coordinates is given below.

$$(1-\varepsilon)\frac{\partial c_i}{\partial t} = \dot{m}_i + (1-\varepsilon)D_h\left[\left(\frac{\partial^2 c_i}{\partial x^2}\right) + \left(\frac{\partial^2 c_i}{\partial y^2}\right)\right] \quad (1)$$

The transient variation of hydride concentration is equal to the sum of hydrogen absorbed and diffused spatially within the bed.

### Absorption Kinetics

Mass of hydrogen absorbed by species 1(NaAlH<sub>4</sub>), 2(Na<sub>3</sub>AlH<sub>6</sub>) and 3(NaH) are given by the following expressions as given below.

$$m_1 = r_{1F}\left[\frac{3c_2}{c_{eqv}} - c_{2sat}\right]\chi_{1F} \quad (p \geq p_{eq1}) \quad (2a)$$

$$m_1 = r_{1B}\left[\frac{c_1}{c_{eqv}}\right]\chi_{1B} \quad (p < p_{eq1}) \quad (2b)$$

$$m_3 = r_{2F}\left[\frac{c_3}{c_{eqv}} - c_{3sat}\right]\chi_{2F} \quad (p \geq p_{eq2}) \quad (2c)$$

$$m_3 = r_{2B}\left[\frac{3c_2}{c_{eqv}}\right]\chi_{2B} \quad (p < p_{eq2}) \quad (2d)$$

$$m_2 = -\frac{1}{3}[m_1 + m_3] \quad (2e)$$

Hydriding and dehydriding rates of reactions 1 and 2 as given by the UTRC kinetic model [11] are given below:

$$r_{1F} = c_{eqv}A_{1F} \exp\left[-\frac{E_{1F}}{RT}\right]\left[\frac{p - p_{eq1}}{p_{eq1}}\right] \quad (3a)$$

$$r_{1B} = -c_{eqv}A_{1B} \exp\left[-\frac{E_{1B}}{RT}\right]\left[\frac{p_{eq1} - p}{p_{eq1}}\right] \quad (3b)$$

$$r_{2F} = -c_{eqv}A_{2F} \exp\left[-\frac{E_{2F}}{RT}\right]\left[\frac{p - p_{eq2}}{p_{eq2}}\right] \quad (3c)$$

$$r_{2B} = c_{eqv}A_{2B} \exp\left[-\frac{E_{2B}}{RT}\right]\left[\frac{p_{eq2} - p}{p_{eq2}}\right] \quad (3d)$$

### Energy Balance

#### Hydride bed

The hydride bed is assumed to be in thermal equilibrium and the heat transfer between the alanate bed and gas is neglected. Convection and radiation effects are also neglected. Energy conservation of hydride bed is expressed as follows.

$$(\rho c_p)_e \frac{\partial T}{\partial t} = k_e \left[ \frac{\partial^2 T}{\partial x^2} + \frac{\partial^2 T}{\partial y^2} \right] - m \Delta H^0 \quad (4)$$

As per the heat equation given above, heat stored in the bed is equal to the sum of net heat transfer in the given spatial coordinates and the sorption heat. As the hydride bed consists of powder particles interspersed with hydrogen, effective thermo-physical properties are used in this equation.

The effective volumetric heat capacity is given by the following equation

$$(\rho c_p)_e = (\varepsilon \rho_h c_{ph} + (1 - \varepsilon) \rho_s c_{ps}) \quad (5)$$

Effective thermal conductivity is given by the following expression.

$$k_e = \varepsilon k_h + (1 - \varepsilon) k_s \quad (6)$$

### **Aluminum structure**

Energy balance of the aluminum structure is given by the following equation.

$$\rho_{Al} (c_p)_{Al} \frac{\partial T}{\partial t} = \nabla \cdot (k_{Al} \nabla T) \quad (7)$$

### **Initial and Boundary conditions**

#### **Initial conditions**

At  $t = 0$

$$c_1 = c_{10} \quad c_2 = c_{20} \quad c_3 = c_{30}; \quad T = T_0 \quad (8)$$

#### **Boundary conditions**

The solid walls are impermeable for mass transfer.

$$\frac{\partial c_i}{\partial r} = 0 \quad (9)$$

The convective condition exists at the heat exchanger walls.

$$-k_e \frac{\partial T}{\partial r} = h_f (T_s - T_f) \quad (10)$$

The rest of the boundaries except heat exchanger walls are treated as adiabatic.

$$-n_s \cdot (-k_e \nabla T_s) = 0 \quad (11)$$

As the thermal resistance between hydride bed and the aluminum structure is assumed to be negligible, heat flux continuity conditions are applied at the respective interface boundaries.

$$-n_s \cdot (-k_e \nabla T_s) = -n_{Al} \cdot (-k_{Al} \nabla T_{Al}) \quad (12)$$

## **4. Simulation Methodology**

As the honey comb based device consists of self-similar hexagonal cells of the given configuration, simulations performed on single cell can be indicative of the device performance. Figure 2 shows the schematic of the hexagonal cell used in simulation. A single cell of ribbed honeycomb can be considered as an assembly of T shaped fins which transfers heat from a location of max temperature

in the porous hydride bed to the cooling tube. The ratios of the linear dimensions of the cell wall and the rib and their corresponding thicknesses can characterize the heat transfer performance of the cell. The sorption performance of individual cells of different length and thickness ratios were modelled and simulated in COMSOL Multiphysics®[12] commercial software.

The 2D geometrical models were created in AutoCAD®. The coupled heat and mass conservation equations in chemical engineering module model hydrogen sorption in the powdery alloy. Unstructured triangular mesh of given element shape and size is generated. Mesh resolution required for simulation is determined using grid independence test. Iterative linear solvers are employed for solving. The post-processing features of this software are used in the results visualization and data processing.

### **Validation of numerical results**

Prior to the parametric study conducted on the storage device, the mathematical model is validated with the experimental data reported by BJ Hardy (2007) [11] as shown in Fig. 3. The results show reasonable agreement for gas pressure of 6.8 M Pa and absorption temperature of 100°C. The above numerical model is used for the heat and mass transfer simulations reported in the present paper.

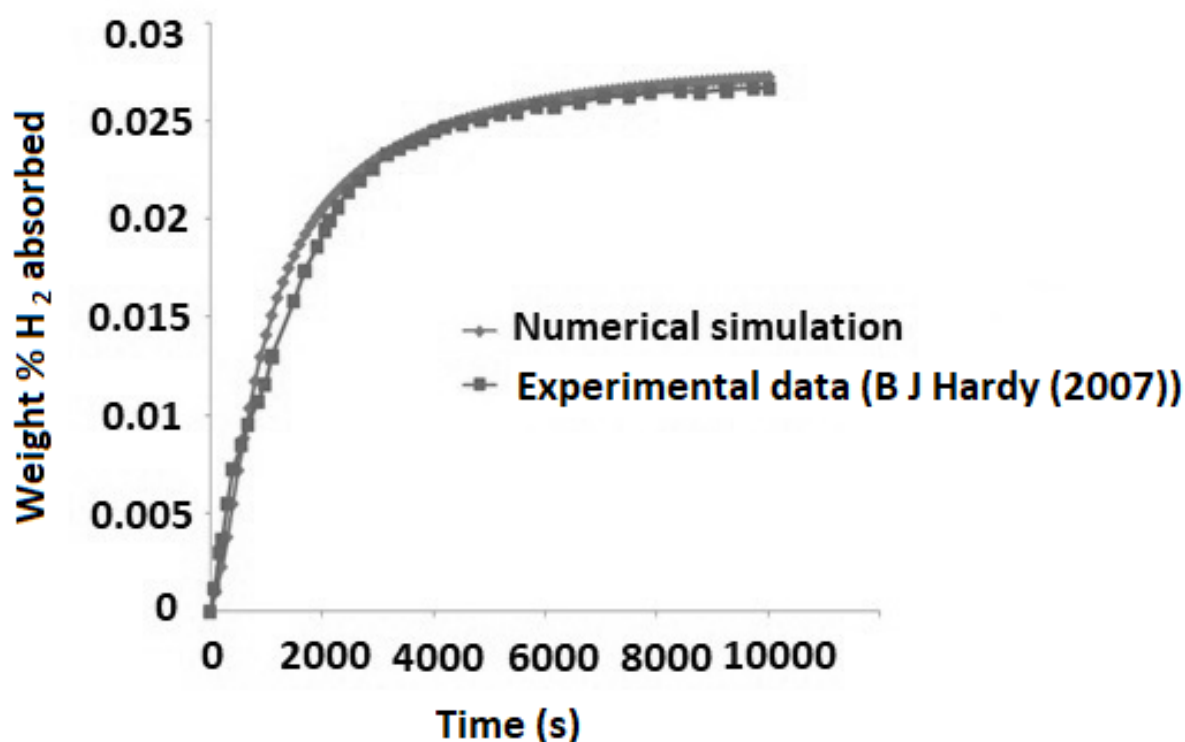


Fig. 3 Comparison of simulation results with experimental data (B J Hardy (2007)) for hydrogen absorption at 6.8 MPa and 100°C

## **5. Results and Discussion**

The device proposed for the study is filled with sodium alanate as the storage material due to its high gravimetric storage capacity, sorption performance and reversibility. The material is well characterized and its hydrogenation is thermally controlled. The thermo-physical properties of materials suggested for the proposed device are given in Table 1. Based on the performance simulations for the parametric ranges given in Table 2, effects of salient controlling parameters on sorption performance of the device are discussed in the following paragraphs.

Table 1. Thermo-physical properties of storage material [11, 13]

Parameter	Value (constant)		
	Sod. alanate	Al	
Thermal conductivity, W/m-K	0.325	160	
Density, kg/m <sup>3</sup>	720	2700	
Specific heat capacity, J/kg-K	820	900	
Activation energy (J/mol) (Rea.1)	Hyd.	80000	-
	Dehyd.	110000	-
Activation energy (J/mol) (Rea.2)	Hyd.	70000	-
	Dehyd.	110000	-
Constants (Rea.1)	$\Delta H_1/R$	-4475	-
	$\Delta S_1/R$	-14.83	-
Constants (Rea. 2)	$\Delta H_2/R$	-6150	-
	$\Delta S_2/R$	-16.22	-
Heat of reaction (Rea. 1) (J/mol)	37000	-	
Heat of reaction (Rea. 2) (J/mol)	47000	-	
Constants in kinetic rate property equations (Eq. 3a -3d and 4a - 4d)	A <sub>1F</sub>	1e8	-
	A <sub>1B</sub>	4e4	-
	A <sub>2F</sub>	1.5e5	-
	A <sub>2B</sub>	6e12	-
	$\chi_{1F}$	2	-
	$\chi_{1B}$	2	-
	$\chi_{2F}$	1	-
	$\chi_{2B}$	1	-

Table 2. Parameter values used in simulation

Parameter	Range
Supply pressure of hydrogen (bar)	100
Coolant temperature (K)	373 K
Void fraction of bed	0.5 (constant)
Tube wall heat transfer coefficient, W/m <sup>2</sup> -K	500 (constant)
Tube diameter, mm	8
Bed thickness, mm	4 - 20
Thickness ratio ( $t_0/t_1$ )	0.25-1

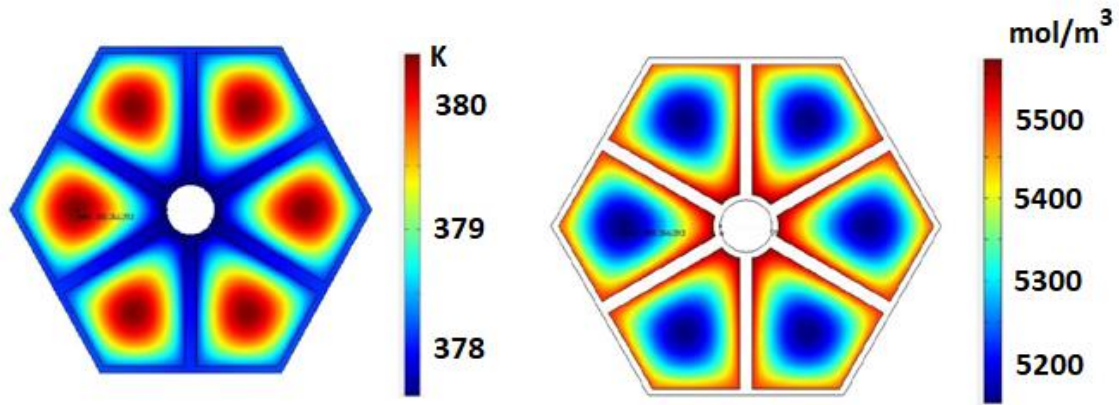


Fig. 4 Spatial variation of temperature and concentration during hydrogenation ( $b=20$  mm,  $t_0/t_1=0.5$ ,  $T_f=373$  K)

Figure 4 shows the spatial variation of temperature and concentration during hydrogenation of the alloy bed embedded within the honeycomb cell. Higher concentration is observed adjacent to the cell walls and the heat exchanger tube. This is due to better heat transfer and low resultant temperature leading to higher differential between gas pressure and equilibrium pressure for absorption.

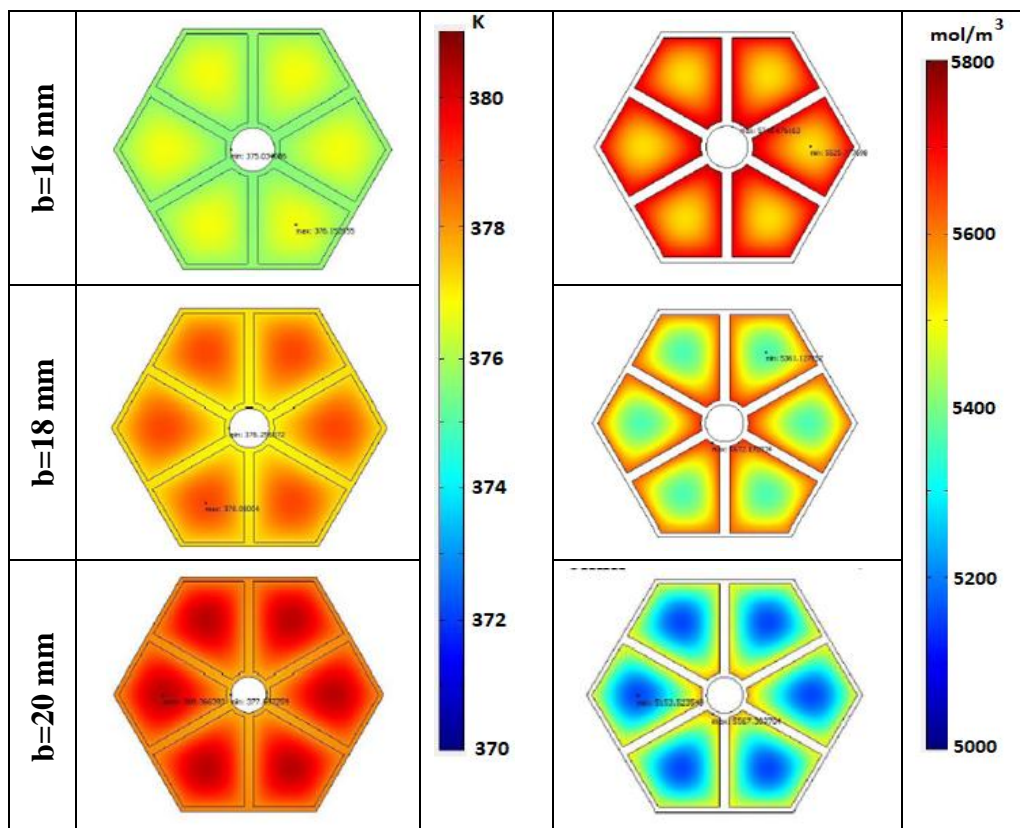


Fig. 5 Effect of bed thickness on spatial variation of temperature and concentration ( $T_f=373$  K,  $t_0/t_1=0.5$ )

Figure 5 shows the effect of bed thickness on the spatial variation of temperature and concentration of the hydride. Bed temperature increases with bed thickness due to higher sorption heat and low thermal conductivity of alloy powder. This leads to correspondingly low hydride concentration. Lowest hydride concentration is observed in regions where temperature is the highest. This is observed in cells with the largest bed thickness and locations farthest from the wall.



Effect of bed thickness on hydrogen sorption with time is shown in Fig. 6. During the initial hydrogenation phase, sorption is vigorous and effect of bed thickness is not evident. However during the later phase, higher bed thickness causes lower rate of hydrogenation due to low heat transfer.

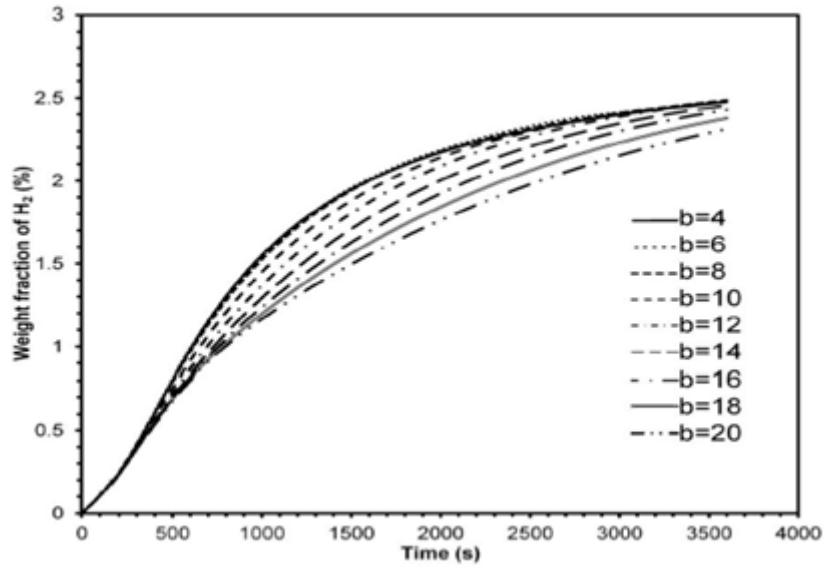


Fig. 6 Effect of bed thickness on hydrogenation ( $T_f=373$  K,  $t_0/t_1=0.5$ )

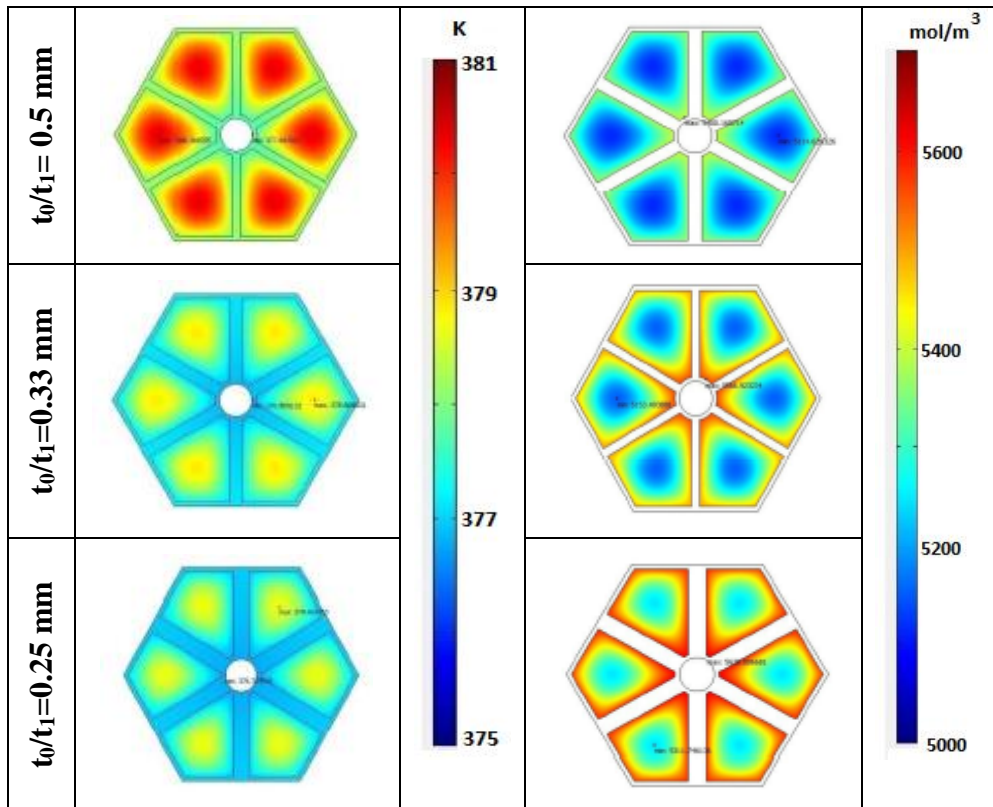


Fig. 7 Effect of thickness ratio ( $t_0/t_1$ ) of the honeycomb cell on spatial variation of bed temperature and concentration ( $T_f=373$  K,  $b=20$  mm)

Figure 7 shows the effect of ratio of the thickness of the cell wall to the rib on hydride concentration and bed temperature. Lower thickness ratio leads to lower bed temperature. This is also evident in Figure 8 which shows the evolution of bed temperature with time at different thickness ratios. Lower

thickness ratio reduces the temperature evolution in the bed. This correspondingly improves the concentration in such cells. The temperature gradient is more drastic where thickness ratio is higher.

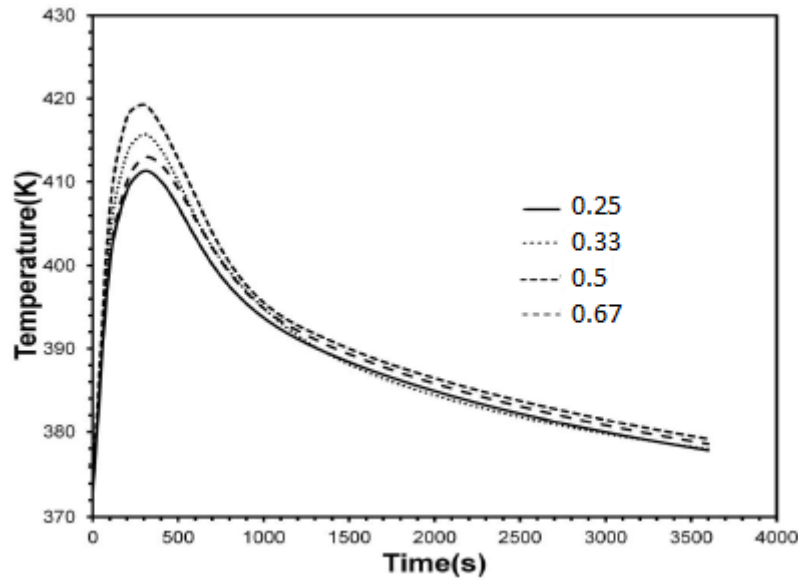


Fig. 8 Effect of thickness ratio ( $t_0/t_1$ ) of the honeycomb cell on average temperature of the hydride bed ( $T_i=373$  K,  $b=20$  mm)

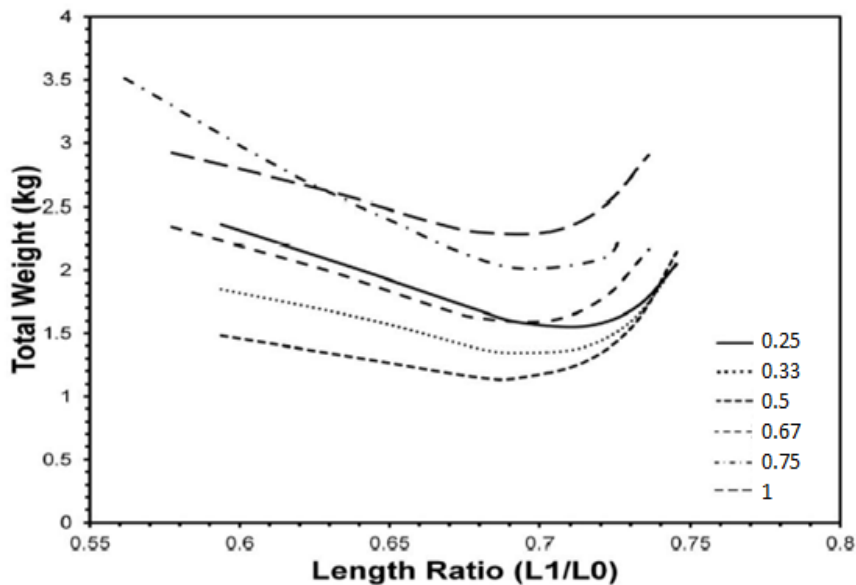


Fig. 9 Effect of length ratio ( $L_1/L_0$ ) on the total weight per given storage capacity and charging time (0.1 kg of  $H_2$  in 600s) of the hydride bed at different thickness ratios ( $t_1/t_0$ )

Effect of ratio of the of side length of the cell wall to the rib length on total weight of the cell for given charging specifications at different thickness ratios is shown in Fig. 9. The weight of the cell decreases progressively with length ratio to a minimum beyond which this increases drastically. This can be due to higher parasitic weight by the honeycomb at smaller length ratios which can decrease to the minimum permitted by the given charging conditions. Beyond this, lower heat transfer can adversely affect sorption performance of the device. The thickness ratio of the cell also shows a similar characteristic for which minimum weight of the cell decreases with increase of thickness ratio upto a global minimum beyond which this increases. This is also attributed by cell heat transfer at a given configuration.

## 6. Conclusions

Numerical simulation of hydrogen sorption in solid state hydrogen storage device embedded with constructal design of aluminum honeycomb is conducted with sodium alanate as the storage medium. Simulation results show the relevance of length and thickness ratios on the weight optimization of the device for the given sorption performance. An optimized constructal network of high conductivity form embedded within the device can achieve given charging performance with the minimum total weight.

## Acknowledgment

This study is supported by the Department of Science and Technology, Govt. of India under MECSP 2017 scheme. The help rendered by Prof. M. P. Maiya, IIT Madras and Dr. K. Balasubramanian, NIFTDC Hyderabad is gratefully acknowledged.

## References

1. Groll M., "Reaction beds for dry sorption machines", *Heat Recovery Systems and CHP*, 13(1993), 341-346.
2. Hardy B.J., Anton D.L., "Hierarchical methodology for modeling hydrogen storage systems. Part I: Scoping models", *International Journal of Hydrogen Energy*, 34(2009a), 2269-2277.
3. Hardy B.J., Anton D.L., "Hierarchical methodology for modeling hydrogen storage systems. Part II: Detailed models", *International Journal of Hydrogen Energy*, 34(2009b), 2992-3004.
4. Raju M., Kumar S., "System simulation modeling and heat transfer in sodium alanate based hydrogen storage systems", *International Journal of Hydrogen Energy*, 36(2011), 1578-1591.
5. Bhouri M., Goyette J., Hardy B. J., Anton D. L., "Numerical modeling and performance evaluation of multi-tubular sodium alanate hydride finned reactor", *International Journal of Hydrogen Energy*, 37(2012), 1551-1567.
6. Bhouri M., Goyette J., Hardy B. J., Anton D. L., "Honeycomb metallic structure for improving heat exchange in hydrogen storage system", *International Journal of Hydrogen Energy*, 36(2011), 6723-6738.
7. Lozano G. A., Eigen N., Keller C., Dornheim M., Bormann R., " Effects of heat transfer on the sorption kinetics of complex hydride reacting systems", *International Journal of Hydrogen Energy*, 34(2009), 1896-1903.
8. Mohan G., Prakash Maiya M., Srinivasa Murthy S., Performance simulation of metal hydride hydrogen storage device with embedded filters and heat exchanger tubes," *International Journal of Hydrogen Energy*, 32(2007), 4978-4987.
9. Mohan G., Prakash Maiya M., Srinivasa Murthy S., "A cell based approach to determine the minimum weight of metal hydride hydrogen storage devices," *ASME 3<sup>rd</sup> International Conference on Energy Sustainability (ES 2009)*, San Francisco, July 19-23. 2009.
10. Sandrock G., Gross K., Thomas G., Jensen C., Meeker D., Takara S., "Engineering considerations in the use of catalyzed sodium alanates for hydrogen storage", *Journal of Alloys and Compounds*, 330-332(2002), 696-701
11. Hardy B. J., 2007, "Integrated hydrogen storage system model," Washington Savanna River Company Document, WSRC-TR-2007-00440, Rev. 0.
12. Comsol Multiphysics User's Guide. Comsol AB, Sweden, 2005.
13. Dedrick D.E., Kanouff M.P., Replogle B. C., Gross K. J., "Thermal properties characterization of sodium alanates", *Journal of Alloys and Compounds*, 389(2005), 299-305.